Journal of Applied Polymer Science

Preparation of Silver Nanoparticle Immobilized Fibrillar Silicate by Poly(dopamine) Surface Functionalization

Ye Fu,[1,2] Guofeng Li,[3] Ming Tian,[2] Xing Wang,[3] Liqun Zhang,[1] Wencai Wang[1,2]

[1]State Key Laboratory of Organic Inorganic Composites, Beijing University of Chemical Technology, Beijing 100029, China
[2]Key Laboratory of Carbon Fiber and Functional Polymers, Ministry of Education, Beijing 100029, China
[3]College of Life Science and Technology, Beijing University of Chemical Technology, Beijing 100029, China
Correspondence to: W. Wang (E-mail: wangw@mail.buct.edu.cn)

Surface modified fibrillar silicate (FS) was prepared by dopamine oxide polymerization and self-assembly of poly(dopamine) (PDA) on the FS surface, presynthesized silver nanoparticles subsequently adhered to the PDA functionalized FS (FS-PDA) surface by simply dipping FS-PDA in silver nanoparticles solution, owing to the metal-binding ability of catechol and nitrogen-containing groups on the PDA coating on the surface of FS. The chemical composition of the modified FS surface was determined by X-ray photoelectron spectroscopy. Surface morphological changes of the FS nanofibers were observed by transmission electron microscopy. The results indicated that the *in situ* spontaneous oxidative polymerization of dopamine on the FS surface and the immobilization of Ag nanoparticles on the surface of FS were successful. The FS-PDA/Ag demonstrated a significant enhancement in antibacterial properties compared to the pristine FS by using *Escherichia coli* as model strain. © 2013 Wiley Periodicals, Inc. J. Appl. Polym. Sci. **2014**, *131*, 39859.

KEYWORDS: nanoparticles; nanowires and nanocrystals; fibers; self-assembly

Received 18 April 2013; accepted 17 August 2013
DOI: 10.1002/app.39859

INTRODUCTION

A chemical approach to construct one-dimensional inorganic nanomaterials-based hybrid nanostructures offers a promising method for functionalizing materials.[1,2] Silver nanoparticles have the remarkable superior optical, catalytic, and antimicrobial properties; they are among the best substrates for surface-enhanced Raman spectroscopy,[3,4] and also exhibit antibacterial properties because of their large surface area and high reactivity.[5] The combination of antibacterial properties and low toxicity for silver nanoparticles has been attracting significant attention.[6–10] Nanocomposites may combine the mechanical properties of a substrate with the properties of nanoparticles to possess properties that are not available to the respective components alone.[11]

Fibrillar silicate (FS) is a kind of nanofiber which is refined from attapulgus clay. Attapulgus clay, commonly called attapulgite after the principal mineral it contains, is a crystalline hydrated magnesium aluminum silicate with a unique chain structure that gives it nanofibrillar micromorphology.[12] The high surface area, thermal resistance, and fibrous morphology of attapulgite provide much potential for diverse applications such as catalyst supports,[13] nanocomposites,[14,15] and environmental absorbents.[16] Surface functionalization of attapulgite has been extensively carried out to modify their intrinsic properties for the applications in various areas.[17] On the other hand, because of the rich surface-plasmon-related light absorption and scattering properties of noble metal nanoparticles, a large number of efforts have been devoted to the assembly of noble metal nanoparticles in order to enhance the amplification of optical signals, including fluorescence,[18–20] Raman scattering,[21–23] and second-harmonic generation,[24] which is useful for medical imaging and diagnostic applications.[25,26] Zhang and coworkers fabricated gold and silver nanoparticles on mesostructured silica nanofibers that were synthesized with a structure-directing agent presence.[27] Because of the inactive surface of inorganic materials and the highly curved surface of this nanoscale substrate with the diameter of 10–20 nm, it is hard to modify and assemble silver nanoparticles on the surface. Until now, few efforts toward such hybrid ultra-fine inorganic nanostructures have focused on silicate or silica nanofibers. Further, the reported synthesis processes are somewhat complicated, so a convenient, inexpensive and environmentally friendly method is desirable.

Poly(dopamine) (PDA) could be formed on a wide range of inorganic and organic materials by *in situ* spontaneous oxidative polymerization of dopamine in alkaline solution at room temperature.[28–30] The *in situ* spontaneous polymerization of dopamine provides the advantages of one-step surface functionalization with simple ingredients, mild reaction

condition, and applicability to various types of materials. More importantly, the PDA layer could be used as a versatile platform for secondary reactions.[31,32] Especially, the metal-binding ability of catechol and nitrogen-containing groups present in the PDA structure may be exploited to immobilize metal particles onto various substrates without conventional environment-unfriendly oxidation and activation-sensitization processes. However, to the best of our knowledge, the preparation of FS-Ag hybrids utilizing this technique has not been explored.

In this work, a PDA assisted method was proposed for silver nanoparticles immobilization on the FS surface. FS was first coated with a PDA layer and silver nanoparticles were then assembled on the surface of the FS-PDA by immersing the FS-PDA into the silver nanoparticles solution. The chemical composition and crystal structure of the as-prepared hybrids were characterized by X-ray photoelectron spectroscopy (XPS) and X-ray diffraction (XRD), respectively. Thermo Gravimetric Analysis (TGA) was used to characterize the thermal stability of FS-PDA and verify the amount of PDA *in situ* spontaneous oxidative polymerized on the FS surface. Surface morphological changes of the FS nanofibers were observed by transmission electron microscopy (TEM). The antimicrobial property enhancement provided by binding of the silver nanoparticles was also demonstrated.

EXPERIMENTAL

Materials

Attapulgite was provided by Jiuchuan Clay Technology Limited Company, Jiangsu, China. FS was refined from attapulgite by soaking it in a sodium hexametaphosphate solution. The dosage of sodium hexametaphosphate is 3% of the weight of attapulgite, with stirring for 30 min at 40°C, followed by vacuum drying prior to use. Dopamine (99%) and Tris(hydroxymethyl)aminomethane (Tris, 99%) were purchased from Alfa Aesar Company, USA. Silver nitrate (99.8%), sodium borohydride, sodium hydroxide, and citric acid were obtained from Beijing Chemical Plant, Beijing, China. All the chemicals were used as received and without further purification.

Dopamine Polymerization on the FS Surface

Dopamine solutions with different concentrations (0.5, 1, 2, and 4 g/L) were prepared by dissolving Tris in different quantities of dopamine-HCl solution. The pH of the dopamine solution was buffered to 8.5. Solution pH was measured by a Mettler Toledo FE-20 pH meter, fitted with a combined glass electrode (0.01 pH units). FS (3 wt %) were dispersed in the dopamine solution by stirring for a predetermined time at 25°C. Then the FS coated with PDA were separated by centrifugation, rinsed thoroughly by ultrasonic with deionized water, and dried in vacuum. The PDA-coated FS will be denoted as FS-PDA-*x* in the subsequent discussion. Where, *x* stands for the concentration of dopamine.

Silver Nanoparticles Immobilization on the FS-PDA Surface

Ag nanoparticles were prepared by reducing $AgNO_3$ with $NaBH_4$ using citrate as a stabilizer. In a typical process, 1 mL $AgNO_3$ solution (0.01*M*) and 1 mL sodium citrate solution (0.01*M*) were first added to 38 mL water, and then 0.25 mL freshly prepared ice-cold $NaBH_4$ solution (0.01*M*) was injected into the solution under vigorous stirring. Silver nanoparticles were formed and used in the following experiment within 24 h. The average diameter of the Ag nanoparticles was (6 ± 2) nm observed by TEM. The FS-PDA-2 (15 mg) was dispersed into 5 mL ethanol by sonication, and then mixed with 35 mL Ag nanoparticle solution. After 30 min, the FS nanofibers coated with Ag nanoparticles were collected by centrifugation and re-dispersed into 35 mL citrate solution (0.01*M*), in order to enhance further adsorption of the Ag nanoparticles onto the FS.[33] For comparison purpose, the pristine FS were also used to prepare FS/Ag hybrids through the same process of FS-PDA/Ag hybrids.

Antibacterial Assay

Escherichia coli (*E. coli*) ATCC 8739 (The Institute of Microbiology, Chinese Academy of Sciences, IMCAS) is used as model strain to investigate the nature of antibacterial ability of FS-PDA/Ag. Samples were made by pressing 5 mg the powder of FS and FS-PDA/Ag on the scissored filter paper. *E. coli* strain was grown overnight in Luria–Bertani (LB) medium (tryptone 10 g/L, yeast extract 5 g/L and NaCl 5 g/L) at 37°C. The bacterial concentrations were dilute (10^5–10^6 CFU/mL) and dispersed uniformly on the surface of LB plate (LB broth with 1.5–2.0% agar). The samples were laid on the top of plate with the surface adhered FS, FS-PDA, and FS-PDA/Ag powder and incubated at 37°C. The FS and FS-PDA samples were used as the control. After 24 h of incubation, the zone of inhibition against the bacteria was measured and compared with control samples.

Characterization

XPS measurements were carried out on an ESCALAB 250 Thermo Electron Corporation with an Al Kα X-Ray source (1486.6 eV) at a constant record ratio of 40. The core-level signals were obtained at a photoelectron takeoff angle of 45° (with respect to the sample surface). The X-ray source was run at a reduced power of 150 W. The powdered samples were pressed into tablets and mounted on the standard sample studs by means of double-sided adhesive tapes. The pressure in the analysis chamber was maintained at 10^{-8} Torr or lower during each measurement. To compensate for surface charging effects, all binding energies (BE's) were referenced to the C 1s hydrocarbon peak at 284.6 eV.

TEM (JEM-3010 electron microscope, JEOL, Japan) was performed on a FEI tacnai G^2 20 STwin TEM. The specimens for TEM observation were prepared by dropping sample suspensions onto carbon membrane support films, and the solvent was allowed to evaporate before observation.

TGA was performed on a STARe system?Mettler Toledo? from 30°C to 800°C at a rate of 10°C/min with a steady nitrogen flow (50 mL/min).

The XRD patterns of the products were recorded on Tecnai $G^2$20 diffractometer with Cu Kα as the radiation source (λ = 0.1541 nm) for a 2θ range of 10° to 90°.

RESULTS AND DISCUSSION

The preparation of FS-PDA-Ag hybrids was carried out in a two step procedure, in which silver nanoparticles immobilization on

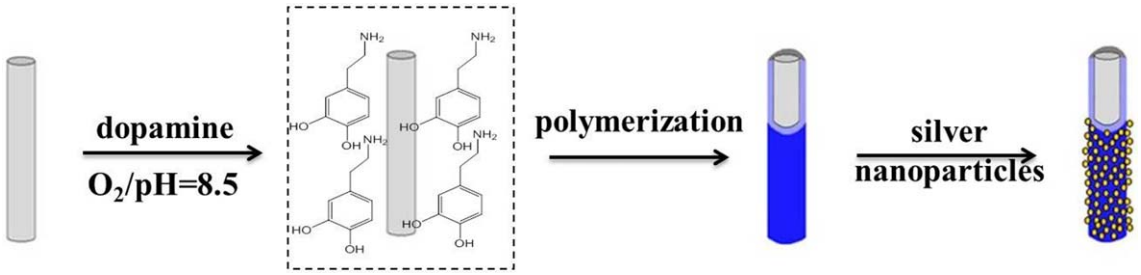

Figure 1. Schematic illustration of the procedure for preparation of the FS-PDA/Ag hybrids. [Color figure can be viewed in the online issue, which is available at wileyonlinelibrary.com.]

the FS surfaces is assisted by bound PDA (Figure 1). The dopamine solution was colorless and transparent. During the *in situ* spontaneous oxidative polymerization of dopamine, the color of solution turned to pink quickly as the catechol was oxidized to benzoquinone, and then the pink solution turned slowly into deep dark, indicating that the polymerization may be followed by reaction in a manner of melanin formation.

Preparation of FS-PDA

XPS was employed to determine the chemical compositions of the surface of as-prepared products. The XPS wide scan spectra of the pristine FS [Figure 2(a)] and FS-PDA [Figure 2(b)] were shown in Figure 2. The pristine FS surface was composed of Si, O, and Mg peaks. The C1s and N 1s peaks were attributed to the organic substances absorbed on FS. The presence of the

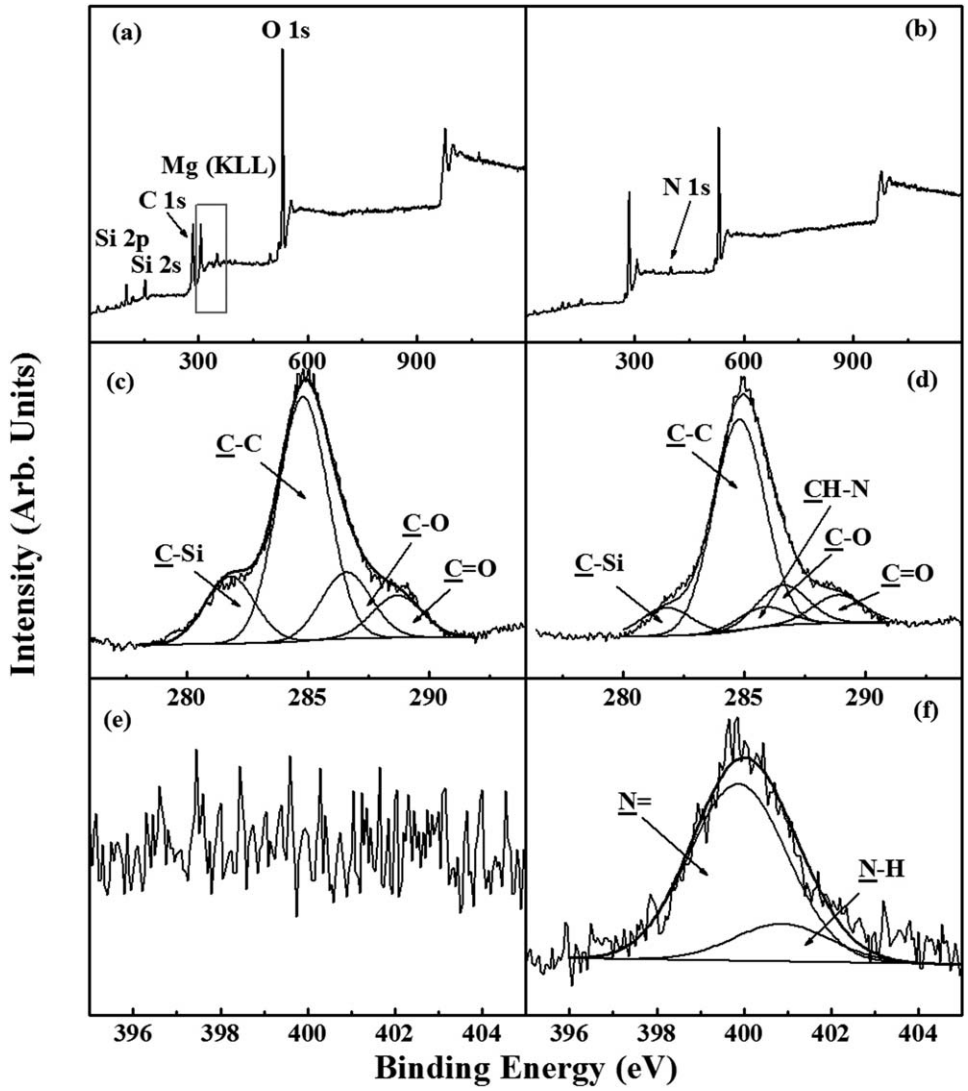

Figure 2. XPS wide scan spectra and C 1s and N 1s core-level spectra of: (a, c, e) pristine FS and (b, d, f) the FS-PDA.

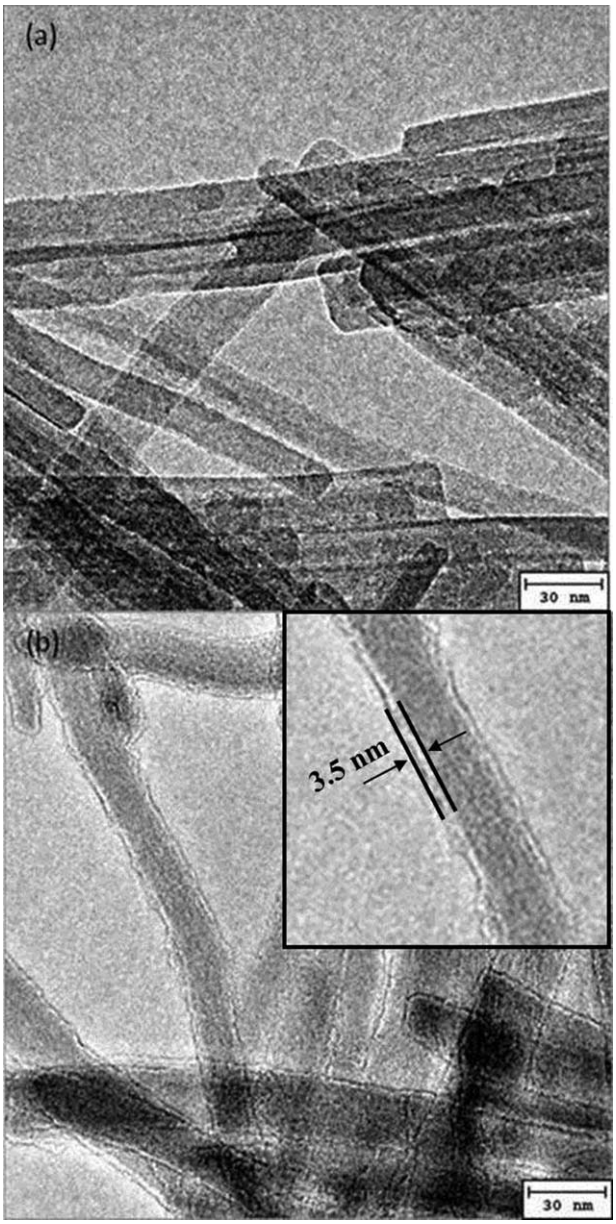

Figure 3. TEM images of: (a) the pristine FS and (b) the FS-PDA-2.

PDA on the FS surface can be deduced from the increase of the peak component at BE of about 400 eV, associated to the nitrogen containing species in PDA. Furthermore, the substantially decreased ration of peak intensity of O 1s to C 1s further confirmed the presence of PDA, associated to the lower mole ratio of oxygen to carbon in PDA. The above results indicated that the *in situ* spontaneous oxidative polymerization of dopamine on the FS surface was successful. The presence of the PDA on the FS surface can be further ascertained by the changes in the XPS C 1s and N 1s core-level line shape. The XPS C1s and N 1s core-level spectra of pristine FS [Figure 2(c,e)] and the FS-PDA [Figure 2(d,f)] were shown in Figure 2, respectively. The C 1s core-level spectrum of the pristine FS can be curved-fitted with four peak components, having BEs at 281.8 eV for the C–Si species, 284.6 eV for the C–H species, at 286.4 eV for the C–O species, and at 288.5 eV for the $N(C{=}O)_2$ species.[34] Deposition of PDA on FS resulted in an additional peak component for C–N (285.6 eV). In addition, the C–Si peak component associated with the FS substrates persists in the curve-fitted C 1s core-level spectra of the FS-PDA surface. This result suggests that the thickness of the deposited PDA is below the probing depth of the XPS technique (about 7.5 nm for an organic matrix). As shown in Figure 2(e), the N 1s core-level spectrum of the pristine FS has no peak. The presence of the deposited dopamine polymer on the FS surface can be deduced from two peak components at the BE of 399.5 eV for the N–H species, which attributed to the amine group of the dopamine and at the BE of 398.5 eV for the N= species [Figure 2(f)].

The morphologies of FS and FS-PDA were investigated by TEM. Figure 3 shows the TEM images of the pristine FS [Figure 3(a)], FS-PDA prepared with the dopamine concentration of 2 g/L [Figure 3(b)]. The fibrillar nanostructure of FS with the diameter of 10-20 nm was observed clearly. From images (b), we could see that FS was coated with uniform PDA layer with a PDA thickness of about 3.5 nm when the concentration of dopamine was 2 g/L.

TGA was used to characterize the thermal stability of FS-PDA and verify the amount of PDA *in situ* spontaneous oxidative polymerized on the FS surface. Figure 4 shows the weight curves (a) and weight loss curve (b) (TGA) of the FS and FS-PDA-*x*. The TGA of the FS had 15.5% weight loss at temperature up to 800 °C. The pure PDA obtained by *in situ* oxidative polymerization of 2.0 g/L of dopamine had about 44.9% weight loss at the temperature up to 800°C, which demonstrated the heat resistance of PDA is quite high. As the weight loss of FS-PDA-0.5, FS-PDA-1, FS-PDA-2, FS-PDA-4 is 20.4%, 22.7%, 26.7%, and 33.2%; it can be calculated that the PDA content of FS-PDA-0.5, FS-PDA-1, FS-PDA-2, FS-PDA-4 is about 10.9%, 16.0%, 24.9%, and 39.3%, respectively. The above results indicate that the thickness and amount of the PDA coating layer increased with the concentration of dopamine, which is in accordance with the TEM results.

Preparation of FS-PDA/Ag Hybrids

The metal-binding ability of catechol and nitrogen-containing groups present in the PDA structure was exploited to immobilize metal particles onto FS-PDA surface. The silver nanoparticles could be absorbed by catechol and nitrogen-containing groups. In this work, we used FS-PDA-2 and FS as materials to prepare FS-PDA/Ag hybrids and FS/Ag hybrids, respectively.

The XPS results of the FS-PDA/Ag hybrids are shown in Figure 5. The strong signal of Ag at BE of about 370 eV in Figure 5(a) demonstrates the presence of silver element. The Ag 3d core-level spectrum shown in Figure 5(b) can be deduced from two peak components with BEs of 368.0 and 374.0 eV for Ag $3d_{5/2}$ and Ag $3d_{3/2}$, respectively. Both of the peaks are attributed to the Ag^0 species, further confirming that the Ag nanoparticles on the surface of the hybrids exist in the zero valent state.

The surface morphologies and distribution of Ag nanoparticles on the FS-PDA surfaces were observed by TEM. For comparison purpose, the Ag nanoparticles deposited on the pristine FS

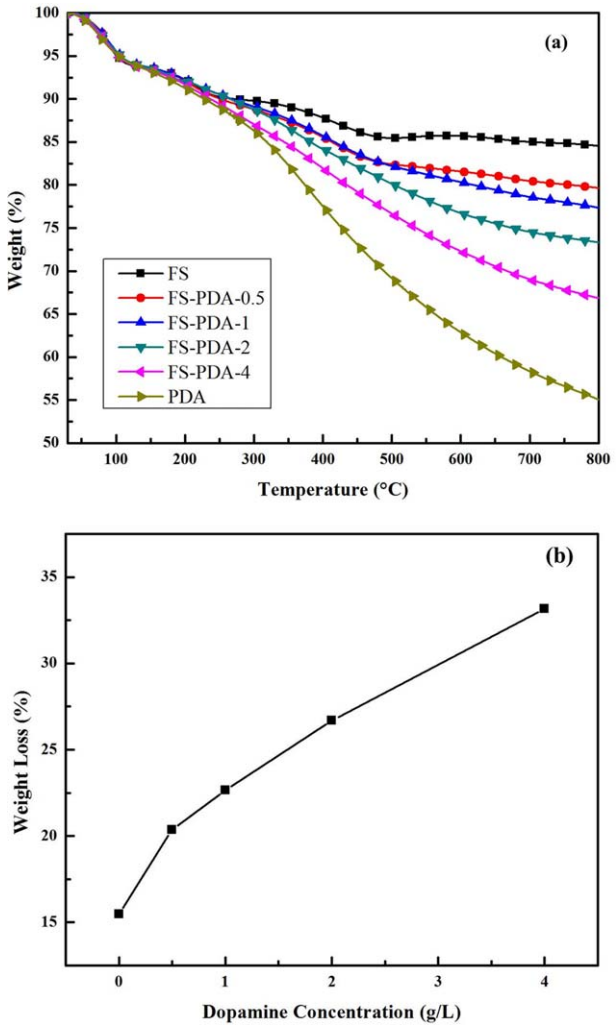

Figure 4. (a) TGA curves of the pristine FS, PDA and FS-PDA; (b) weight loss of the pristine FS, PDA and FS-PDA during the TGA. [Color figure can be viewed in the online issue, which is available at wileyonlinelibrary.com.]

surfaces [Figure 6(a)] and FS-PDA surfaces [Figure 6(b)] under the same condition are presented. Figure 6(b) evidenced the high-density and homogeneously dispersed spherical silver nanoparticles on the surface of the FS-PDA. The diameter of Ag nanoparticles was about 10 nm, and the space between silver nanoparticles was within 10 nm. However, there are no Ag nanoparticles observed on the pristine FS [Figure 6(a)], which further indicates that the modification of FS by PDA is the key contribution for immobilizing Ag nanoparticles on the surface of FS.

Figure 7 shows the XRD patterns of the pristine FS [Figure 7(a)] and the FS-PDA [Figure 7(b)] and the FS-PDA/Ag hybrids [Figure 7(c)]. The peak positions 2θ = 19.7, 27.5, 34.6, and 42.5 are exactly the same in the pristine FS and the FS-PDA, which indicates the FS crystal structure does not change after PDA successfully polymerized on the FS. The peak positions 2θ = 13.6 and 16.4 correspond to the Si–O–Si crystalline layer.[35] The FS-PDA/Ag hybrids show new peaks at 2θ of 38.1°, 44.3°, 64.4°, and 77.4°, assigned to the (111), (200), (220), and (311) phases of the face-centered cubic (fcc) crystal structure of silver nanoparticles, respectively (JCPDS card No 4-783). The above results accord well with the presence of Ag estimated from XPS measurement.

All FS-PDA/Ag hybrids used for analysis were rinsed by vigorous ultrasonic and the Ag nanoparticles on the surface of FS-PDA did not fall off, which were observed by SEM. The above results indicated that the interaction between the silver nanoparticles and the FS-PDA surface was relatively strong. The strong interaction was presumed to be very important for the formation of homogeneously dispersed Ag nanoparticles on the FS-PDA surface.

Antibacterial Activity of FS-PDA/Ag

Figure 8 shows the results of inhibition zone used to evaluate the antimicrobial activity of FS-PDA/Ag. Approximately 105-106 CFU/mL of *E. coli* was first plated on nutrient agar and the samples were laid for 24 h at 37°C. The samples of (a) pristine FS and (b) FS-PDA failed to show an inhibition zone, however, a clear inhibition zone was observed for the sample of (c) FS-PDA/Ag. It indicates that the antimicrobial activity of a surface can be easily increased by performing deposition of silver nanoparticles on PDA-coated surface and cannot be achieved by purely modified PDA layer. Parikh[36] produced Ag-filled wound

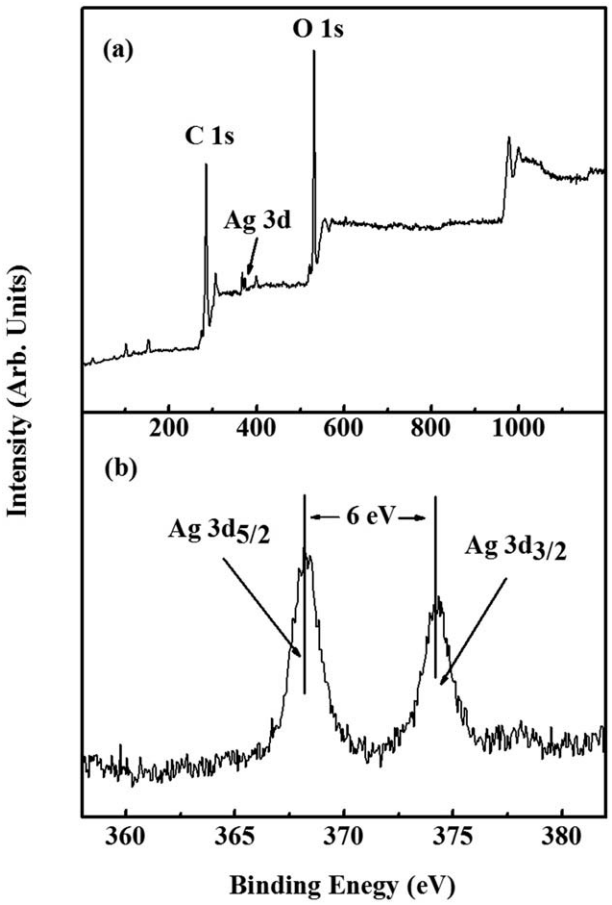

Figure 5. XPS (a) wide scan spectra and (b) Ag 3d spectra of the FS-PDA/Ag hybrids.

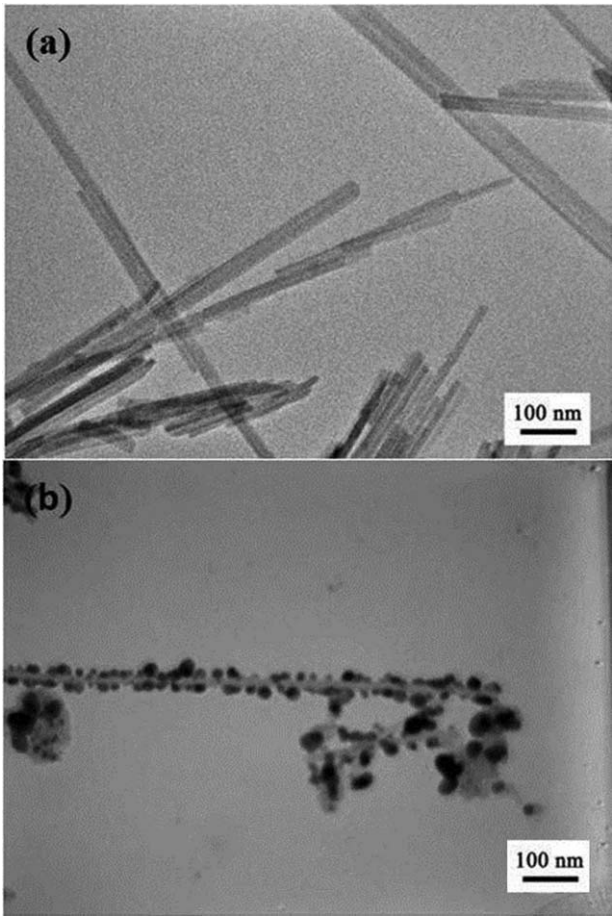

Figure 6. TEM images of: (a) the FS/Ag hybrids and (b) the FS-PDA/Ag hybrids.

dressings and they evaluated the antimicrobial activity of wound dressings against *Staphylococcus aureus* and *Klebsiella pneumonia*. As a consequence, FS-PDA/Ag has the potential application as antimicrobial materials.

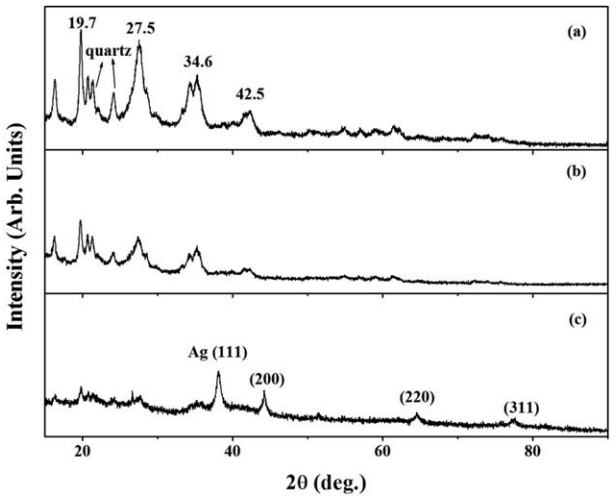

Figure 7. XRD patterns of: (a) the pristine FS, (b) the FS-PDA and (c) the FS-PDA/Ag hybrids.

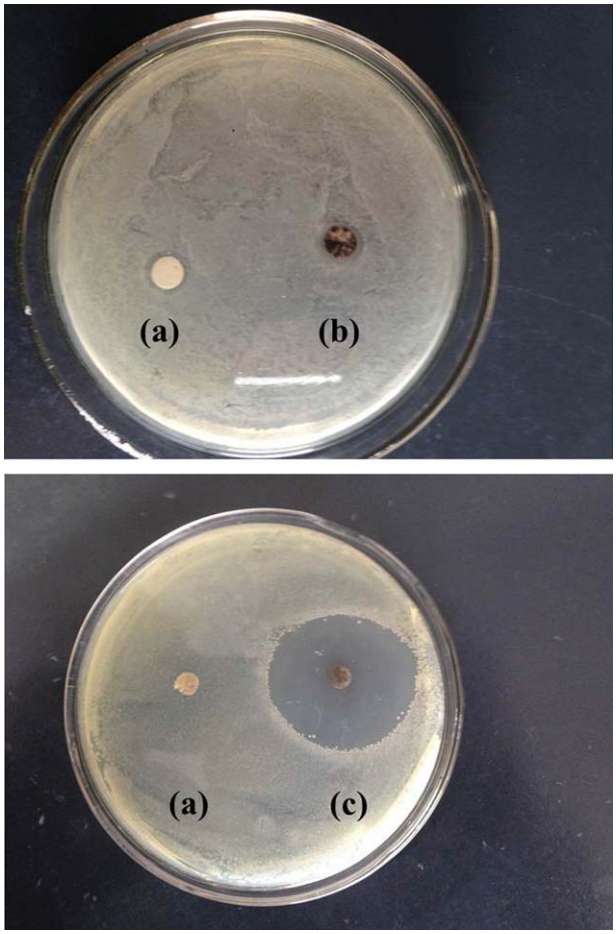

Figure 8. Antimicrobial efficiency of the inoculated (a) FS, (b) FS-PDA and (c) FS-PDA/Ag against *E. coli*. [Color figure can be viewed in the online issue, which is available at wileyonlinelibrary.com.]

CONCLUSION

A PDA-assisted procedure for silver nanoparticles immobilization on FS surface was demonstrated. PDA layers with high surface coverage were formed on FS by *in situ* spontaneous oxidative polymerization of dopamine. The PDA functional layer not only improved the dispersion of FS in aqueous solutions, but also was used as a platform for subsequent silver nanoparticle immobilization. The thermal property of FS-PDA/Ag was determined, which investigated the outstanding thermal stability of PDA layer. Finally, antimicrobial activity of the produced FS-PDA/Ag was evaluated against *E. Coli*, which shows that the nanocomposite fibers were effective against *E. Coli*. These fibers may be used to cover the wounds especially burn wounds or medical packaging.

ACKNOWLEDGMENTS

The authors sincerely appreciate the financial supports from the Natural Science Foundation of China (Grant No. 51073013, 51373010), the Program for New Century Excellent Talents in University (NCET-11-0562), and the Natural Science Foundation of Beijing City (No. 2122049).

REFERENCES

1. Byeon, J. H.; Kim, J. W. *J. Colloid Interface Sci.* **2010**, *348*, 649.
2. Jiang, Y.; Lu, Y. L.; Zhang, L. Q.; Liu, L.; Dai, Y. J.; Wang, W. C. *J. Nanopart. Res.* **2012**, *6*, 938.
3. Schueler, P. A.; Ives, J. T.; DeLaCroix, F.; Lacy, W. B.; Becker, P. A.; Li, J.; Caldwell, K. D.; Drake, B.; Harris, J. M. *Anal. Chem.* **1993**, *65*, 3177.
4. Lu, L. H.; Wang, H. S.; Zhou, Y. H.; Xi, S. Q.; Zhang, H. J.; Hu, J. W.; Zhao, B. *Chem. Commun.* **2002**, *2*, 144.
5. Sawhney, A. P. S.; Condon, B.; Simgh, K. V.; Pang, S. S.; Li, G.; Hui, D. *Text. Res. J.* **2008**, *78*, 731.
6. Niño-Martínez, N.; Martínez-Castañón, G. A.; Aragón-Piña, A.; Martínez-Gutierrez F.; Martínez-Mendoza J. R.; and Facundo Ruiz. *Nanotechnology* **2008**, *19*, 065711/1.
7. Alt, V.; Bechert, T.; Steinrucke, P. Wagenerc, M.; Seideld, P.; Dingeldeind, E.; Domanne, E, and Schnettlera, R. *Biomaterials* **2004**, *25*, 4383.
8. Sukdeb, P.; Yu, K. T.; Song, J. M. *Appl Environ. Micr.* **2007**, *73*, 1712.
9. AshaRani, P. V.; Grace, L. K. M.; Manoor, P. H.; Suresh, V. *ACS Nano.* **2009**, *3*, 279.
10. Varun, S.; Megan, M. M.; Blake, R. P.; Ayusman, S. *J. Am. Chem. Soc.* **2006**, *128*, 9798.
11. Lin, Y.; Watson, K. A.; Fallbach, M. J.; Ghose, S.; Smith, J. G.; Delozier, D. M.; Cao, W.; Crooks, R. E.; Connell, J. W. *ACS Nano* **2009**, *3*, 871.
12. Bradley, W. F. *Am. Mineralofist.* **1940**, *25*, 405.
13. Cao, J. L.; Shao, G. S.; Wang, Y.; Liu, Y.; Yuan, Z. Y. *Catal.Commun.* **2008**, *9*, 2555.
14. Liu, Y.; Liu, P.; Su, Z.; Li, F.; Wen, F. *Appl. Surf. Sci.* **2008**, *255*, 2020.
15. Pan, B.; Ren, J.; Yue, Q.; Liu, B.; Zhang, J.; Yang, S. *Polym. Compos.* **2009**, *30*, 147.
16. Wang, W.; Zheng, Y.; Wang, A. *Polym. Adv. Technol.* **2008**, *19*, 1852.
17. Liu, P. *Appl. Clay Sci.* **2007**, *38*, 64.
18. Aslan, K.; Leonenko, Z.; Lakowicz, J. R.; Geddes, C. D. *J. Phys. Chem. B* **2005**, *109*, 3157.
19. Aslan, K.; Lakowicz, J. R.; Geddes, C. D. *J. Phys. Chem. B* **2005**, *109*, 6247.
20. Zhang, J.; Matveeva, E.; Gryczynski, I.; Leonenko, Z.; Lakowicz, J. R. *J. Phys. Chem. B* **2005**, *109*, 7969.
21. Freeman, R. G.; Grabar, K. C.; Allison, K. J.; Bright, R. M.; Davis, J. A.; Guthrie, A. P.; Hommer, M. B.; Jackson, M. A.; Smith, P. C.; Walter, D. G.; Natan, M. J. *Science* **1995**, *267*, 1629.
22. Tao, A.; Kim, F.; Hess, C.; Goldberger, J.; He, R. R.; Sun, Y. G.; Xia, Y. N.; Yang, P. D. *Nano Lett.* **2003**, *3*, 1229.
23. Orendorff, C. J.; Gole, A.; Sau, T. K.; Murphy, C. J. *Anal. Chem.* **2005**, *77*, 3261.
24. Hayakawa, T.; Usui, Y.; Bharathi, S.; Nogami, M. *Adv. Mater.* **2004**, *16*, 1408.
25. Shafer Peltier, K. E.; Haynes, C. L.; Glucksberg, M. R.; Van Duyne, R. P. *J. Am. Chem. Soc.* **2003**, *125*, 588.
26. Zhang, X. Y.; Young, M. A.; Lyandres, O.; Van Duyne, R. P. *J. Am. Chem. Soc.* **2005**, *127*, 4484.
27. Zhang, S. Z.; Ni, W. H.; Kou, X. S.; Yeung, M. H.; Sun, L. D.; Wang, J. F.; Yan, C. H. *Adv. Funct. Mater.* **2007**, *17*, 3258.
28. Messersmith, P. B. *Science* **2008**, *319*, 1767.
29. Brubaker, C. E.; Messersmith, P. B. *Langmuir*, **2012**, *28*, 2200.
30. Kang, S. M.; Rho, J.; Choi, I. S.; Messersmith, P. B.; Lee, H. *J. Am. Chem. Soc.* **2009**, *131*, 13224.
31. Ni, K.; Lu, H.; Wang, C.; Black, K. L. C.; Wei, D.; Ren, Y.; Messersmith, P. B. *Biotechnol. Bioeng.* **2012**, *109*, 2970.
32. Sun, I. C.; Eun, D. K.; Na, J. K.; Lee, S.; Kim, I. J.; Youn, I. C.; Ko, C. Y.; Kim, H. S.; Lim, D.; Choi, K.; Messersmith, P. B.; Park, T. G.; Kim, C. Y.; Kwon, I. C.; Kim, K.and Ahn C. H. *Chem. Eur. J.*, **2009**, *15*, 13341.
33. Grabar, K. C.; Smith, P. C.; Musick, M. D.; Davis, J. A.; Walter, D. G.; Jackson, M. A.; Guthrie, A. P.; Natan, M. J. *J. Am. Chem. Soc.* **1996**, *118*, 1148.
34. Liu, P. *Appl. Clay Sci.*, **2007**, *35*, 11.
35. Fan, Q. H.; Shao, D. D.; Hu, J.; Wu, W. S.; Wang, X. K. *Surf. Sci.* **2008**, *602*, 778.
36. Parikh, D. V.; Fink, T.; DeLucca, A. J.; Parikh, A. D. *Text. Res. J.* **2011**, *81*, 494.